Available online at www.sciencedirect.com
SCIENCE DIRECT®
ELSEVIER
International Journal of Solids and Structures 43 (2006) 5403–5420
INTERNATIONAL JOURNAL OF SOLIDS and STRUCTURES
www.elsevier.com/locate/ijsolstr

Discussion

Use of magnetorheological elastomer in an adaptive sandwich beam with conductive skins. Part II: Dynamic properties

G.Y. Zhou *, Q. Wang

Department of Mechanical, Materials and Aerospace Engineering, University of Central Florida, Orlando, FL 32816, USA

Received 14 April 2005; received in revised form 28 June 2005
Available online 12 September 2005

Abstract

The second part of this research is to present the field-dependant dynamic property of a sandwich beam with conductive skins and a soft core composed of a magnetorheological elastomer (MRE) part and two non-MRE parts. The MRE part of the core is configured to operate in shear mode and hence the dynamic properties of the sandwich beam can be controlled by magnetic fields due to the field-dependant shear modulus of MRE material. According to the analytical solution for the magnetoelastic loads applied to conductive deformable bodies presented in the first part, the model of the proposed sandwich beam is developed via Hamilton principle. A simply supported MRE-based sandwich beam excited by a vertical force distributed uniformly in a narrow region around the center of the beam is simulated. The anti-resonant frequencies and the resonant frequencies are found to change with the applied magnetic field up to 30%. The procedure to seek the optimal length of MRE part is also presented. Although MRE is a soft material with shear modulus about 0.4 Mpa, this research indicates that the sandwich configuration can well utilize the controllable property of MRE to design applicable smart devices with controllable stiffness.

Keywords: Sandwich beam; Semi-active vibration control; Magnetorheological elastomer

1. Introduction

Owing to regular chain-like structures formed by ferrous particles and embedded in rubber matrix, magnetorheological elastomer (MRE) is a composite with field-dependant modulus. MRE is cured under strong magnetic fields and hence the formed chain-like structures are orientated along the magnetic field. When magnetic fields are applied parallel to such chain-like structures in application, the bulk shear modulus

* Corresponding author. Tel.: +1 407 207 7426.
E-mail address: gangyi@gmail.com (G.Y. Zhou).

0020-7683/$ - see front matter © 2005 Published by Elsevier Ltd.
doi:10.1016/j.ijsolstr.2005.07.044

Nomenclature

T kinetic energy
U strain energy
V work due to external forces and the magnetoelastic loads acting on the skins
δ variation operator
ρ_j ($j = $ t, b, c) mass density of the top (t) and bottom (b) skins and the core (c), respectively
u_j ($j = $ t, b, c) longitudinal displacement in the top (t) and bottom (b) skins and the core (c)
w_j ($j = $ t, b, c) transverse displacement in the top (t) and bottom (b) skins and the core (c)
V_j ($j = $ t, b, c) volume of the top (t) and bottom (b) skins and the core (c)
u_{oj} ($j = $ t, b) horizontal displacement of the mid-line of the top (t) and bottom (b) skins
w_{oj} ($j = $ t, b) vertical displacement of the mid-line of the top (t) and bottom (b) skins
Z_j ($j = $ t, b) half thickness of the skins
D_j ($j = $ t, b) thickness of the skins
σ_{xxj} ($j = $ t, b, c) longitudinal normal stress in the top (t) and bottom (b) skins and the core (c)
ε_{xxj} ($j = $ t, b, c) longitudinal strain in the top (t) and bottom (b) skins and the core (c)
τ_{xzc} shear stress in the core
τ abbreviation of τ_{xzc}, see Eq. (21)
γ_{xzc} shear strain in the core
q_j ($j = $ t, b) vertical external distributed forces at the top (t) and bottom (b) skins
n_j ($j = $ t, b) horizontal external distributed forces at the top (t) and bottom (b) skins
m_j ($j = $ t, b) moments external distributed loads at the top (t) and bottom (b) skins
$\mathbf{f}^{je}$ ($j = $ t, b) Lorenz body force inside the top (t) and bottom (b) skins
B_0 modulus of the magnet induction of applied magnetic fields perpendicular to sandwich beams
μ_0 magnetic permeability in free spaces
μ_{ej} ($j = $ t, b) permeability of the top (t) and bottom (b) skins
n_j^{Lor} ($j = $ t, b) equivalent Horizontal force induced by Lorenz body force at the top (t) and bottom (b) skins
m_j^{Lor} ($j = $ t, b) equivalent moments induced by Lorenz body force at the top (t) and bottom (b) skins
σ_{zx}^{mj} ($j = $ t, b) surface stress on the top (t) and bottom (b) skins caused by Maxwell's stress jump
m_j^{Max} equivalent moments induced by Maxwell's stress jump at the top (t) and bottom (b) skins
n_j^m equivalent horizontal force induced by magnetoelastic loads at the top (t) and bottom (b) skins. See Eq. (13a)
m_j^m equivalent moments induced by magnetoelastic loads at the top (t) and bottom (b) skins. See Eq. (13b)
H width of the sandwich beam
L length of the sandwich beam
c thickness of the core
S_j ($j = $ t, b, c) cross-sectional area of the top (t) and bottom (b) skins and the core (c)
N_{xxj} ($j = $ t, b) average normal stress on the top (t) and bottom (b) skins. See Eq. (20)
M_{xxj} ($j = $ t, b) average stress couples on the top (t) and bottom (b) skins. See Eq. (20)
G_c transverse shear modulus of the core
E_j ($j = $ t, b, c) Young's modulus of the top (t) and bottom (b) skins and the core (c)
I_j ($j = $ t, b) flexure moment of the top (t) and bottom (b) skins and the core (c)
k_{ap} apparent stiffness of a simply supported sandwich beam. See Eq. (42)

J	relative change of the apparent stiffness, k_{ap}, between zero-field shear modulus and maximum field-induced shear modulus of the MRE core
$\hat{x}$	unit vector of x coordinate
ω	angular frequency
γ_{MRE}	relative change of the shear modulus of the MRE part of the core induced by magnetic fields

*Remarks: $()'$, and $()''$ denote the first order derivative and second order derivative with respect to time respectively; $()_{,x}$ denotes the partial derivative with respect to x coordinate; the superscript "∧" indicates the Fourier transform with respect to time

of MRE can be changed up to 60% of the zero-field shear modulus due to the magnetic interaction between the particles inside the chains (Zhou, 2003). Due to its stable, reversible and rapid responded field-controllable characteristics, MRE is a much more promising material in developing semi-active devices.

MRE was introduced by Shiga (Shiga et al., 1995) and Jolly (Jolly et al., 1996) nearly 10 years ago when many research efforts were still paid on MRF and MRF-based damping devices. Previous researches on MRE were focused on its field-dependant shear modulus heavily. The field-dependant shear modulus was investigated experimentally by shearing MRE (Jolly et al., 1996; Ginder et al., 1999) on material test system or measuring the vibration of sandwich cantilever (Demchuk and Kuzmin, 2002). Employing dipole model and finite element method, Davis (1999) reported the maximum change of the dynamic shear modulus of MRE is about 50% which occurs when the volume fraction is 27%. This conclusion was verified experimentally by Zhou through free vibration experiment (Zhou, 2003). Zhou further reported that such field-dependant shear modulus became null when the deformation frequency was beyond several hundreds Hertz (Zhou, 2004). Devices utilizing such field-dependant shear property were also introduced (Badolato and Pawlowski, 2003; Zhou and Wang, 2005, in press). Recently, the relaxation behavior (Schlotter et al., 2002; Zhou and Jiang, 2004) and dynamic tension behavior (Zhou and Li, 2003) of MRE were also reported. Though MRE exhibits controllable and stable properties, it is rather soft and its zero-field shear modulus is as lower as 0.4 MPa (Davis, 1999). This does hinder its application since the area of the magnetic poles cannot be manufactured very large. Sandwich configuration provides an alternative to apply the field-controllable property of MRE to engineering applications.

Sandwich beams have been in use for many years in industries, especially in aerospace engineering, due to their high strength–mass ratio (Librescu and Hause, 2000). A typical construction of a beam consists of two skins and a core. Numerous references can be found in literature covering the debonding problem (Frostig, 1992), buckling problem (Librescu and Hause, 2000), and dynamic mechanical problem of curved (Bozhevolnaya and Frostig, 1997) or non-curved beams (Frostig and Baruch, 1994). Many works proved that the transverse flexibility of the core affects the overall behaviors of sandwich beams, such as stresses and displacements (Librescu and Hause, 2000; Frostig and Baruch, 1994). Theories describing the bulk property of sandwich beams based on different assumptions of displacement fields inside cores have been developed. In the references (Frostig, 1992; Frostig and Baruch, 1994), those theories were reviewed and compared. Among these theories, the high-order theory developed by Frostig (Frostig and Baruch, 1994) was successful for the analysis of such sandwich beams with transversely flexible cores. Thus, this theory will be used for the present analysis.

As the further approach of the investigation on MRE-based sandwich beam with non-conductive skins (Zhou and Wang, 2005, in press), this article provides a fundamental analysis on how magnetic fields change the dynamic property of the MRE-based sandwich beam with conductive skins. Different from the case of non-conductive skins, the magnetic field will both change the mechanical property of MRE and generate magnetoelastic loads subjected to the skins. Based on the analytical solution for the magnetoelastic loads

applied to conductive deformable bodies presented in the first part, the mathematical formulation and the boundary conditions for a general case will be presented. The shear modulus of the core is assumed to be a distributing function along the longitudinal direction since the MRE part of the core is affected by the magnetic field while the non-MRE parts are not. Numerical results for a simply supported beam are presented to study the field-controllable dynamic property of the proposed sandwich beam excited by a vertical force at the center of the beam. The procedure to seek the optimal length of the MRE part to yield maximum controllable range of the bulk dynamic flexure rigidity is also conducted. Since skins strengthen bulk flexure rigidities of sandwich beams, this sandwich configuration would lead to applicable semi-active devices by taking the advantage of field-dependant property of MRE.

2. Mathematical formulation

The proposed sandwich beam consists of two conductive skins and a soft core, which is composed of an MRE part and two non-MRE parts. The MRE part is configured with the chain-like structures embedded in the material perpendicular to the skins. The applied magnetic field is parallel to such chain-like structures and is perpendicular to the skins. Under dynamic deformations, motion-induced eddy current will be generated on the skins. Thus, the magnetic field near the skins will be disturbed and magnetoelastic loads will be applied to the skins. As a result, the bulk dynamic flexure rigidity is affected by the applied magnetic field through the field-dependant shear modulus of the MRE part of the core and the magnetomechanical coupling mechanism of the conductive skins. In our analysis, we assume the field-disturbance due to motion-induced eddy current on skins is extremely small compared with the applied magnetic field. That is the transverse shear modulus of the MRE part is only a function of the applied magnetic field and the MRE part. On the other hand, due to the bulk magnetic permeability of MRE is not very high, the motion-induced eddy current on the skins is only associated with the applied magnetic field. In summary, the above two assumptions indicates the field-related mechanical property of the skins and the MRE part can be analyzed separately. It should be mentioned the shear modulus of MRE changes linearly with the strength of the magnetic field till magnetic saturation occurs (Zhou, 2003, 2004). Thus, in the following analysis, only the relative change of the shear modulus of the MRE part is used to denote the effect of magnetic fields on the core.

The mathematical formulation consists of the derivation of the governing field equations of motion and the corresponding boundary conditions for conductive skins and flexible core. They are derived through the Hamilton principle by seeking the extremum of the Lagrangian that consists of the kinetic, strain energy and the work caused by the external force and magnetoelastic loads. Figs. 1 and 2 present the illustration of the proposed sandwich beams and the geometry for analysis. The Lagrangian expression for the sandwich is given as

$$\int_{t_1}^{t_2} \delta(-T + U + V)\mathrm{d}t = 0 \tag{1}$$

where T is the kinetic energy, U is the strain energy, V is the work due to external forces and the magnetoelastic loads acting on the skins, t is the time coordinate between t_1 and t_2, and δ is the variation operator.

2.1. The kinetic energy

The first variation of the kinetic energy for sandwich beam is expressed as

$$\delta T = \int_{v_t} (\rho_t u_t' \delta u_t' + \rho_t w_t' \delta w_t')\mathrm{d}v + \int_{v_b} (\rho_b u_b' \delta u_b' + \rho_b w_b' \delta w_b')\mathrm{d}v + \int_{v_c} (\rho_c u_c' \delta u_c' + \rho_c w_c' \delta w_c')\mathrm{d}v \tag{2}$$

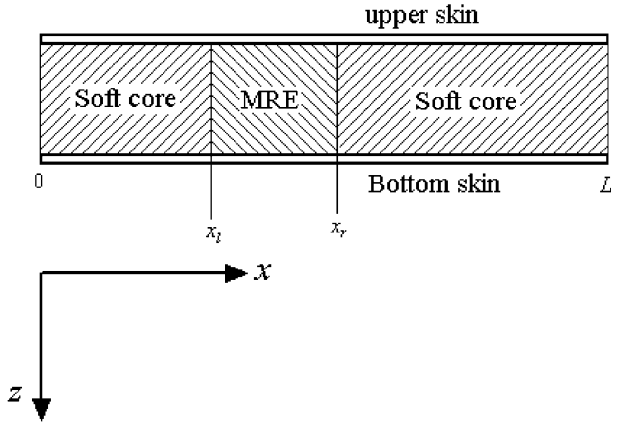

Fig. 1. Illustration of the proposed sandwich beam.

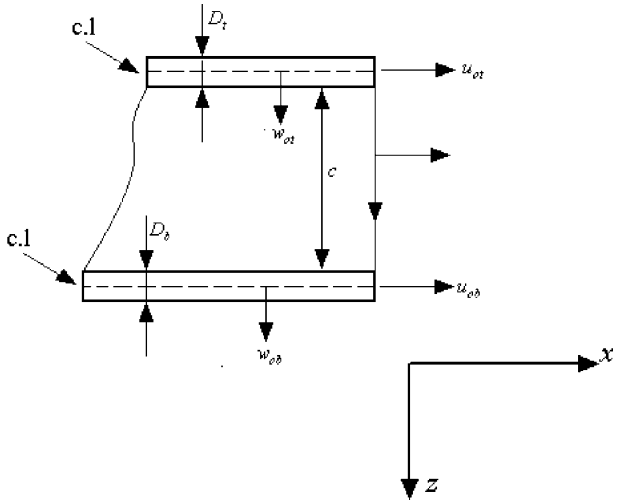

Fig. 2. Geometry of the proposed sandwich beam.

where ρ_j ($j = \mathrm{t}, \mathrm{b}, \mathrm{c}$) is the mass density of the top and bottom skins and the core, respectively; u_j, w_j ($j = \mathrm{t}, \mathrm{b}, \mathrm{c}$) are the displacement in longitudinal and vertical direction, respectively, of the skins and the core; the prime denotes the first derivative respect to the time coordinate; V_j ($j = \mathrm{t}, \mathrm{b}, \mathrm{c}$) is the volume of the top and bottom skins and the core.

After conducting integration by parts with respect to the time coordinate and employing homogeneous conditions for the displacement and velocity at $t = t_1, t_2$, the following relation for the first variation of the kinetic energy is obtained

$$\int_{t_1}^{t_2} \delta T \,\mathrm{d}t = -\int_{t_1}^{t_2} \left[\int_{v_\mathrm{t}} (\rho_\mathrm{t} u_\mathrm{t}'' \delta u_\mathrm{t} + \rho_\mathrm{t} w_\mathrm{t}'' \delta w_\mathrm{t}) \mathrm{d}v + \int_{v_\mathrm{b}} (\rho_\mathrm{b} u_\mathrm{b}'' \delta u_\mathrm{b} + \rho_\mathrm{b} w_\mathrm{b}'' \delta w_\mathrm{b}) \mathrm{d}v + \int_{v_\mathrm{c}} (\rho_\mathrm{c} u_\mathrm{c}'' \delta u_\mathrm{c} + \rho_\mathrm{c} w_\mathrm{c}'' \delta w_\mathrm{c}) \mathrm{d}v \right] \mathrm{d}t \tag{3}$$

where $()''$ denotes the second derivative with respect to time.

Based on Frostig's high-order theory, the soft core is considered as a medium which transfers its inertial loads to the skins rather than resisting them by itself. This consideration indicates the wave-like behavior in the vertical and horizontal directions of the core is prevented. Thus, the acceleration and the velocity in the vertical direction of the core are assumed to have the shape of the static deformation fields. The static displacements field throughout the height of the core is nonlinear, especially in the vicinity of concentrated loads and supports. However, under distributed loads, these nonlinearities are so small that a linear distribution can be used instead without loss of accuracy (Frostig and Baruch, 1994). It should be emphasized that this simplification is employed only for the inertial participation effects of the core. Thus, the displacement inside the core follows the following equations:

$$w''_{\mathrm{c}}(x,z,t) = \frac{\left[w''_{o\mathrm{b}} - w''_{o\mathrm{t}}\right]z}{c} + w''_{o\mathrm{t}} \tag{4a}$$

$$u''_{\mathrm{c}}(x,z,t) = \frac{\left[u''_{o\mathrm{b}} + Z_{\mathrm{b}}w''_{o\mathrm{b},x} - u''_{o\mathrm{t}} + Z_{\mathrm{t}}w''_{o\mathrm{t},x}\right]z}{c} + u''_{o\mathrm{t}} - Z_{\mathrm{t}}w''_{o\mathrm{t},x} \tag{4b}$$

where u_{oj} and w_{oj} ($j = \mathrm{t}, \mathrm{b}$) are the horizontal and vertical displacement of the mid-line, respectively, of the skins; Z_j ($j = \mathrm{t}, \mathrm{b}$) is the half thickness of the skins; $(\,)_{,x}$ denotes a derivative with respect to x.

2.2. The strain energy

The first variation of the strain energy in terms of stress and strain is given as

$$\delta U = \int_{v_{\mathrm{t}}} \sigma_{xxt}\delta\varepsilon_{xxt}\,\mathrm{d}v + \int_{v_{\mathrm{b}}} \sigma_{xxb}\delta\varepsilon_{xxb}\,\mathrm{d}v + \int_{v_{\mathrm{t}}} (\sigma_{zzc}\delta\varepsilon_{zzc} + 2\tau_{xzc}\delta\gamma_{xzc})\mathrm{d}v \tag{5}$$

where σ_{xxj} and ε_{xxj} ($j = \mathrm{t}, \mathrm{b}, \mathrm{c}$) are the longitudinal normal stress and strains, respectively; τ_{xzc} and γ_{xzc} are the shear stress and shear strain in the core.

The kinematics relations for the skins, assuming small linear deformations, are

$$\varepsilon_{xxj} = u_{oj,x} - z_j w_{oj,xx} \quad (j = \mathrm{t}, \mathrm{b}) \tag{6}$$

where z_j ($j = \mathrm{t}, \mathrm{b}$) is the local coordinate of the skins.

The kinematics relations for the core are

$$\varepsilon_{zzc} = w_{\mathrm{c},z} \tag{7a}$$

$$\gamma_{xzc} = \frac{1}{2}(u_{\mathrm{c},z} + w_{\mathrm{c},x}) \tag{7b}$$

where $(\,)_{,z}$ denotes a derivative with respect to z.

2.3. The work by external forces

The first variation of the external energy can be expressed as

$$\delta V = -\int_0^L (q_{\mathrm{t}}\delta w_{\mathrm{t}} + n_{\mathrm{t}}\delta u_{\mathrm{t}} + m_{\mathrm{t}}\delta w_{\mathrm{t},x} + q_{\mathrm{b}}\delta w_{\mathrm{b}} + n_{\mathrm{b}}\delta u_{\mathrm{b}} + m_{\mathrm{b}}\delta w_{\mathrm{b},x})\mathrm{d}x \tag{8}$$

where q_j, n_j and m_j ($j = \mathrm{t}, \mathrm{b}$) are the vertical, horizontal and moments external distributed loads respectively at the top (t) and bottom (b) skins.

2.4. The magnetoelastic loads on the conductive skins

The magnetoelastic loads, referring to the Lorenz body force and the surface force caused by the Maxwell's stress jump on the surface of the conductive skins, will be subjected to the vibrating conductive skins due to the motion-induced eddy current. When the vibrating skin is exposed to the applied magnetic field perpendicularly, the Lorenz body force and the surface force caused by the jumps of the Maxwell's stress tensor on the surface have been obtained analytically in the first part of the research. The results will be listed below.

For a thin-beam immersed in an applied steady magnetic field along the thickness direction, the induced magnetic field inside the perfectly electro-conductive medium is

$$\mathbf{f}^{j\mathrm{e}} = \frac{B_0^2}{\mu_{ej}}(u_{oj,xx} - z_j w_{oj,xxx})\hat{x} \tag{9}$$

where $\mathbf{f}^{j\mathrm{e}}$ ($j = \mathrm{t}, \mathrm{b}$) is the Lorenz body force, μ_{ej} ($j = \mathrm{t}, \mathrm{b}$) is the permeability of the skins, and B_0 is the modulus of the magnetic induction of the applied magnetic field, which is perpendicular to the sandwich beam.

The Lorenz body force will induce horizontal force and moments distributed loads as follows:

$$n_j^{\mathrm{Lor}} = \frac{B_0^2 H D_j}{\mu_{ej}} u_{oj,xx} \tag{10a}$$

$$m_j^{\mathrm{Lor}} = -\frac{B_0^2 H}{\mu_{ej}} \frac{D_j^3}{12} w_{oj,xxx} \tag{10b}$$

The stress on the surface of the beam, which is caused by the jumps of Maxwell's stress tensor, is given as

$$\sigma_{zx}^{mj} = \frac{B_0^2}{\mu_0}\left(\frac{\pi}{2\ln\frac{x}{L-x}} u_{oj,x} - \frac{D_j}{2\pi} w_{oj,xx} \ln\frac{x}{L-x} + w_{oj,x}\right) \tag{11}$$

where σ_{zx}^{mj} ($j = \mathrm{t}, \mathrm{b}$) is the shear stress on the upper and lower skin respectively.

The surface force will induce moments distributed loads, which are

$$m_j^{\mathrm{Max}} = \frac{B_0^2 H D_j}{\mu_0}\left(\frac{\pi}{2\ln\dfrac{x}{L-x}} u_{oj,x} - \frac{D_j}{2\pi} w_{oj,xx} \ln\frac{x}{L-x} + w_{oj,x}\right) \tag{12}$$

Thus, the magnetoelastic loads applied to the conductive beam will be equivalent to the following horizontal force distribution and the distributed moments are expressed as

$$n_j^m = n_j^{\mathrm{Lor}} = \frac{B_0^2 H D_j}{\mu_{ej}} u_{oj,xx} \tag{13a}$$

$$\begin{aligned} m_j^m &= m_j^{\mathrm{Max}} + m_j^{\mathrm{Lor}} \\ &= \frac{B_0^2 H D_j}{\mu_0}\left(\frac{\pi}{2\ln\dfrac{x}{L-x}} u_{oj,x} - \frac{D_j}{2\pi} w_{oj,xx} \ln\frac{x}{L-x} + w_{oj,x}\right) - \frac{B_0^2 H}{\mu_{ej}} \frac{D_j^3}{12} w_{oj,xxx} \end{aligned} \tag{13b}$$

2.5. The governing equation

The governing equations are derived by substituting the above Eqs. (2–13) into Eq. (1). After conducting integration by parts with respect to x and z and some mathematical operations and algebraic manipulations, the governing equations are obtained as

$$\delta u_{0t}: \quad \frac{S_c\rho_c u''_{ob}}{6}+\frac{D_b}{12}S_c\rho_c w''_{ob,x}+\frac{S_c\rho_c u''_{ot}}{3}-\frac{D_t S_c\rho_c w''_{ot,x}}{6}+\rho_t S_t u''_{ot}-n^m_t-n_t-H\tau_{xzc}(0)-N_{xxt,x}=0 \tag{14}$$

$$\delta u_{0b}: \quad \frac{S_c\rho_c u''_{ob}}{3}+\frac{S_c\rho_c D_b w''_{ob,x}}{6}+\frac{S_c\rho_c u''_{ot}}{6}-S_c\rho_c\frac{D_t}{12}w''_{ot,x}+\rho_b S_b u''_{ob}-n^m_b-n_b+H\tau_{xzc}(c)-N_{xxb,x}=0 \tag{15}$$

$$\delta w_{0t}: \quad S_c\rho_c\frac{D_t}{12}u''_{ob,x}+S_c\rho_c\frac{D_t D_b}{24}w''_{ob,xx}+S_c\rho_c\frac{D_t u''_{ot,x}}{6}-(S_c\rho_c+\rho_t S_t)\frac{D_t^2}{12}w''_{ot,xx}+\left(\frac{S_c\rho_c}{3}+\rho_t S_t\right)w''_{ot}+S_c\rho_c\frac{w''_{ob}}{6}-q_t+m^m_{t,x}+m_{t,x}-H\sigma_{zzc}(0)-H\tau_{xzc,x}(0)\frac{D_t}{2}-M_{xxt,xx}=0 \tag{16}$$

$$\delta w_{0b}: \quad -\frac{S_c\rho_c D_b u''_{ob,x}}{6}-(S_c\rho_c+\rho_b S_b)\frac{D_b^2}{12}w''_{ob,xx}-\frac{D_b}{12}S_c\rho_c u''_{ot,x}+\frac{D_b D_t}{24}S_c\rho_c w''_{ot,xx}+\left(\frac{S_c\rho_c}{3}+\rho_b S_b\right)w''_{ob}+\frac{S_c\rho_c w''_{ot}}{6}-q_b+m^m_{b,x}+m_{b,x}+H\sigma_{zzc}(c)-H\tau_{xzc,x}(c)\frac{D_b}{2}-M_{xxb,xx}=0 \tag{17}$$

$$\delta w_c: \quad \sigma_{zzc,z}+\tau_{xzc,x}=0 \tag{18}$$

$$\delta u_c: \quad \tau_{xzc,z}=0 \tag{19}$$

where H is the width of the sandwich beam, D_j ($j=$ t, b) are the thickness of the top and bottom skin; S_j ($j=$ t, b, c) are the cross-sectional area of the top and bottom skins and the core respectively; N_{xxj} and M_{xxj} ($j=$ t, b) are the average normal stress and stress couples defined by

$$N_{xxj}=H\int_{-z_j}^{z_j}\sigma_{xxj}\,dz \quad \text{and} \quad M_{xxj}=H\int_{-z_j}^{z_j}\sigma_{xxj}z\,dz \tag{20}$$

The shear stress in the core, from Eq. (19), is uniform through the height of the core and is only the function of x coordinate. Thus, τ is just a function of x and can be expressed by

$$\tau(x,z)=\tau(x) \tag{21}$$

The constitutive equations of the core are

$$\tau(x)=G_c\gamma_{xzc} \quad \text{and} \quad \sigma_{zzc}=E_c w_{c,z} \tag{22}$$

where G_c and E_c are the shear modulus and Young's modulus of the core respectively.

It should be stressed for MRE material, the transverse shear modulus is a function of applied magnetic field when the deformation frequency is under 300 Hz (Zhou, 2004) while the Young's modulus changes slightly in such frequency range (Zhou and Li, 2003). Since we only consider the case of deformation frequency under 300 Hz, G_c is a function of x while E_c is a constant.

Through Eqs. (18) and (22), the normal stress inside the core can be obtained as

$$\sigma_{zzc}(z=0)=\frac{E_c(w_{ob}-w_{ot})}{c}+\frac{\tau_{,x}}{2}c \tag{23}$$

$$\sigma_{zzc}(z=c)=\frac{E_c(w_{ob}-w_{ot})}{c}-\frac{\tau_{,x}}{2}c \tag{24}$$

The constitutive of the skins leads to

$$N_{xxj} = E_j S_j u_{oj,x} \tag{25}$$

$$M_{xxj} = -E_j I_j w_{oj,xx} \tag{26}$$

where $E_j I_j = H E_j \frac{D_j^3}{12}$ ($j = \mathrm{t}, \mathrm{b}$) is the flexural rigidities.

By substituting Eqs. (23)–(26) into Eqs. (14)–(17), the dynamic governing equations of a sandwich beam with soft core can be expressed in terms of the vertical deformations, w_{ot} and w_{ob}, the horizontal deformations, u_{ot} and u_{ob}, and the shear stress in the core, τ. Thus, there are four linear differential equations but with five independent functions. The additional equation, derived from Eqs. (18) and (19) by using Eq. (22), reads

$$\frac{\tau}{G_c} c - \frac{\tau_{,xx} c^3}{12 E_c} - \frac{c + D_b}{2} w_{ob,x} - \frac{c + D_t}{2} w_{ot,x} - u_{ob} + u_{ot} = 0 \tag{27}$$

The solution for a simply supported sandwich beam governed by Eqs. (14)–(17) and (27) will be presented in the next subsection.

2.6. Solution for simply supported beam

Applying Fourier transform to the above five equations yields

$$-\omega^2\left(\frac{S_c\rho_c}{3} + \rho_t S_t\right)\hat{u}_{ot} - \frac{\omega^2 S_c\rho_c \hat{u}_{ob}}{6} - H\hat{\tau} + \omega^2 \frac{D_t S_c \rho_c \hat{w}_{ot,x}}{6} - \omega^2 \frac{D_b}{12} S_c \rho_c \hat{w}_{ob,x} - E_t S_t \hat{u}_{ot,xx} = \hat{n}_t + \hat{n}_t^m \tag{28}$$

$$-\omega^2 \frac{S_c\rho_c \hat{u}_{ot}}{6} - \omega^2\left(\frac{S_c\rho_c}{3} + \rho_b S_b\right)\hat{u}_{ob} + H\hat{\tau} + \omega^2 S_c\rho_c \frac{D_t}{12}\hat{w}_{ot,x} - \omega^2 \frac{S_c\rho_c D_b \hat{w}_{ob,x}}{6} - E_b S_b \hat{u}_{ob,xx} = \hat{n}_b + \hat{n}_b^m \tag{29}$$

$$-\left(\frac{\omega^2 S_c\rho_c}{3} + \omega^2\rho_t S_t - H\frac{E_c}{c}\right)\hat{w}_{ot} - \left(\frac{\omega^2 S_c\rho_c}{6} + H\frac{E_c}{c}\right)\hat{w}_{ob} - \omega^2 S_c\rho_c \frac{D_t \hat{u}_{ot,x}}{6} - \omega^2 S_c\rho_c \frac{D_t}{12}\hat{u}_{ob,x} - \frac{c + D_t}{2} H\hat{\tau}_{,x} + (S_c\rho_c + \rho_t S_t)\frac{D_t^2}{12}\hat{w}_{ot,xx} - \omega^2 S_c\rho_c \frac{D_t D_b}{24}\hat{w}_{ob,xx} + E_t I_t \hat{w}_{ot,xxxx} = \hat{q}_t - \hat{m}_{t,x}^m - \hat{m}_{t,x} \tag{30}$$

$$-\left(\omega^2 \frac{S_c\rho_c}{6} + H\frac{E_c}{c}\right)\hat{w}_{ot} - \left(\omega^2 \frac{S_c\rho_c}{3} + \omega^2\rho_b S_b - H\frac{E_c}{c}\right)\hat{w}_{ob} + \omega^2 \frac{S_c\rho_c D_b}{6}\hat{u}_{ob,x} + \omega^2 \frac{D_b}{12} S_c\rho_c \hat{u}_{ot,x} - H\frac{c + D_b}{2}\hat{\tau}_{,x} - \omega^2 \frac{D_b D_t}{24} S_c\rho_c \hat{w}_{ot,xx} + \omega^2 (S_c\rho_c + \rho_b S_b)\frac{D_b^2}{12}\hat{w}_{ob,xx} + E_b I_b \hat{w}_{ob,xxxx} = \hat{q}_b - \hat{m}_{b,x}^m - \hat{m}_{b,x} \tag{31}$$

$$\hat{u}_{ot} - \hat{u}_{ob} + \frac{c}{G_c}\hat{\tau} - \frac{c + D_t}{2}\hat{w}_{ot,x} - \frac{c + D_b}{2}\hat{w}_{ob,x} - \frac{c^3}{12 E_c}\hat{\tau}_{,xx} = 0 \tag{32}$$

where the superscript "$\wedge$" denotes the Fourier transformed function and ω is the angular frequency.

The boundary conditions for a simply supported beam are listed below. The vertical displacement of the skins at the two ends should be zero, which yields

$$\hat{w}_{oj}(x = 0) = 0 \tag{33a}$$

and

$$\hat{w}_{oj}(x = L) = 0 \tag{33b}$$

The flexural torque at the two ends should be balanced by the moments induced by magnetoelastic loads. From Eq. (13b), the boundary condition at the two ends is thus derived

$$\left(1+\frac{6D_jB_0^2}{\mu_0\pi E_jD_j^2}\ln\frac{x}{L-x}\right)\frac{\partial^2\hat{w}_{oj}}{\partial x^2}=\frac{12B_0^2}{\mu_0E_jD_j^2}\frac{\partial\hat{w}_{oj}}{\partial x}-\frac{B_0^2}{\mu_{ej}E_j}\frac{\partial^3\hat{w}_{oj}}{\partial x^3} \tag{34}$$

(rewrite it as "because" cannot me a main sentence) To satisfy the above equation, the following conditions must be enforced:

$$\hat{w}_{oj,xx}(x=0)=0 \tag{35a}$$

and

$$\hat{w}_{oj,xx}(x=L)=0 \tag{36b}$$

And the average normal stresses of the skin at the two ends should be balanced by the Lorenz force, which yields

$$\hat{u}_{oj,x}(x=0)=\frac{B_0^2HD_j}{\mu_{ej}E_j}\hat{u}_{oj,xx}(x=0) \tag{37a}$$

and

$$\hat{u}_{oj,x}(x=L)=\frac{B_0^2HD_j}{\mu_{ej}E_j}\hat{u}_{oj,xx}(x=L) \tag{38b}$$

Since $B_0<1$ T, the coefficient of $\frac{B_0^2HD_j}{\mu_{ej}E_j}$ would be extremely small such that the right-hand-side of the above two equations can be neglected. Thus, we have

$$\hat{u}_{oj,x}(x=0)=0 \tag{39a}$$

and

$$\hat{u}_{oj,x}(x=L)=0 \tag{39b}$$

From Eqs. (30) and (32), the boundary of the conductive skins exposed to (do not understand) field perpendicularly can be replaced by that of a pure (simply is one word) supported beam.

The normal stresses on the side surfaces at $x=0$ and $x=L$ should be zero, which yields

$$\hat{\tau}_{,x}(x=0)=0 \tag{40a}$$

and

$$\hat{\tau}_{,x}(x=L)=0 \tag{40b}$$

By the boundary condition of Eqs. (33), (35), and (39), series expression for the displacement distribution of the sandwich beam with simply supported boundary conditions at the skins can be expressed as follows:

$$\hat{u}_{o\mathrm{t}}=\sum_{k=1}^{\infty}a_k^{u\mathrm{tc}}\cos\frac{k\pi x}{L} \tag{41a}$$

$$\hat{u}_{o\mathrm{b}}=\sum_{k=1}^{\infty}a_k^{u\mathrm{bc}}\cos\frac{k\pi x}{L} \tag{41b}$$

$$\hat{w}_{o\mathrm{t}}=\sum_{k=1}^{\infty}a_k^{w\mathrm{ts}}\sin\frac{k\pi x}{L} \tag{41c}$$

$$\hat{w}_{ob} = \sum_{k=1}^{\infty} a_k^{wbs} \sin\frac{k\pi x}{L} \tag{41d}$$

$$\hat{\tau} = \sum_{k=1}^{\infty} a_k^{\tau c} \cos\frac{k\pi x}{L} \tag{41e}$$

where $a_k^j (j = utc, ubc, wts, wbs, \tau c)$ are coefficients.

The coefficients in Eqs. (41a)–(41e) can be obtained through Eqs. (28)–(32) by Galerkin method.

3. Numerical simulations

In the following numerical simulations, the dimensions and material properties of the sandwich beam are given as follows. The width of the beam, H, is set to be $0.1L$; the thicknesses of the top and bottom skins, D_t and D_b, are all set to be 0.1 mm; The Young's modulus of the skins, E_t and E_b, are 72 GPa; the densities of the skins, ρ_t and ρ_b, are 2700 kg/m^3; the zero-field shear modulus of MRE and the shear modulus of the non-MRE soft core are 0.388 MPa; the shear modulus of MRE is assumed to be changed up to 60% of zero-field value by the applied magnetic field, which follows the material parameter of MRE in Davis' study (Davis, 1999); the Young's modulus of the MRE part, which is assumed to be unchanged with the applied magnetic field (Zhou and Li, 2003), and the non-MRE part are set to be 1.7 MPa; the density of the core, including MRE part and the non-MRE part, is 1100 kg/m^3; the thickness of the core is 2 mm. The simulations will be focused in the frequency rang of 0 Hz $\leqslant \frac{\omega}{2\pi} \leqslant$ 300 Hz because the field-depended characteristic of shear modulus of MRE vanishes as frequency goes higher (Zhou, 2004).

All the external forces are set to be zero except the vertical force subjected to the top skin, q_t. q_t is further assumed to be a harmonic force distributing uniformly in the interval of $\frac{L}{2} - \frac{L}{2000} \leqslant x \leqslant \frac{L}{2} + \frac{L}{2000}$. Thus, the displacements and the shear stress in the core can be obtained through the above analysis.

The first 20 terms in series expression of Eqs. (32) and (33) are employed in the simulation. The apparent stiffness at $x = \frac{L}{2}$, which is the center of external force distribution, can be defined by

$$k_{ap}(\gamma_{GMRE}, \omega) = \left| \frac{\hat{F}(\omega)}{\hat{w}_{ot}\left(\omega, \frac{L}{2}\right)} \right| \tag{42}$$

where $\hat{F}(\omega)$ is the Fourier transform of the applied vertical force; γ_{GMRE} is the magnetic-induced relative change of the shear modulus of MRE core located at $x_l \leqslant x \leqslant x_r$. It should be stressed k_{ap} is the only parameter used in our study to reveal the controllability of the proposed sandwich beam.

The maximum value of γ_{GMRE} is 0.6 occurring at the magnetic saturation. To simplify our simulation, the magnetic saturation inside the MRE is assumed to occur at $B_0 = 1$ T. This assumption is reasonable since it agrees well with the material parameter of MRE used in our previous experimental works (Zhou, 2003, 2004). Before magnetic saturation, B_0 is found to be associated with γ_{GMRE} linearly (Zhou, 2003). Thus, γ_{GMRE} can be used to denote the magnetic field induction hereafter.

Fig. 3 presents the curves of $\log_{10} k_{ap}$ against $\frac{\omega}{2\pi}$ at different γ_{MRE}, when $L = 15$ cm and the core are assumed to be composed of MRE completely. The three curves are associated with $\gamma_{MRE} = 0$, $\gamma_{MRE} = 0.3$ and $\gamma_{MRE} = 0.6$ respectively. On the curves, the peaks denote the anti-resonant frequencies, where the induced vertical displacement at $x = \frac{L}{2}$ approaches zero, and the lower-most points denote the resonant frequencies, where the induced vertical displacement at $x = \frac{L}{2}$ goes toward infinite. In other words, the stiffness of the beam at $x = \frac{L}{2}$ is much higher at anti-resonant frequency and is much lower at resonant frequency. From the curves, the anti-resonant frequencies and the resonant frequencies both increase with the shear modulus of MRE core. The maximum change of the anti-resonant frequencies and the resonant frequencies is above

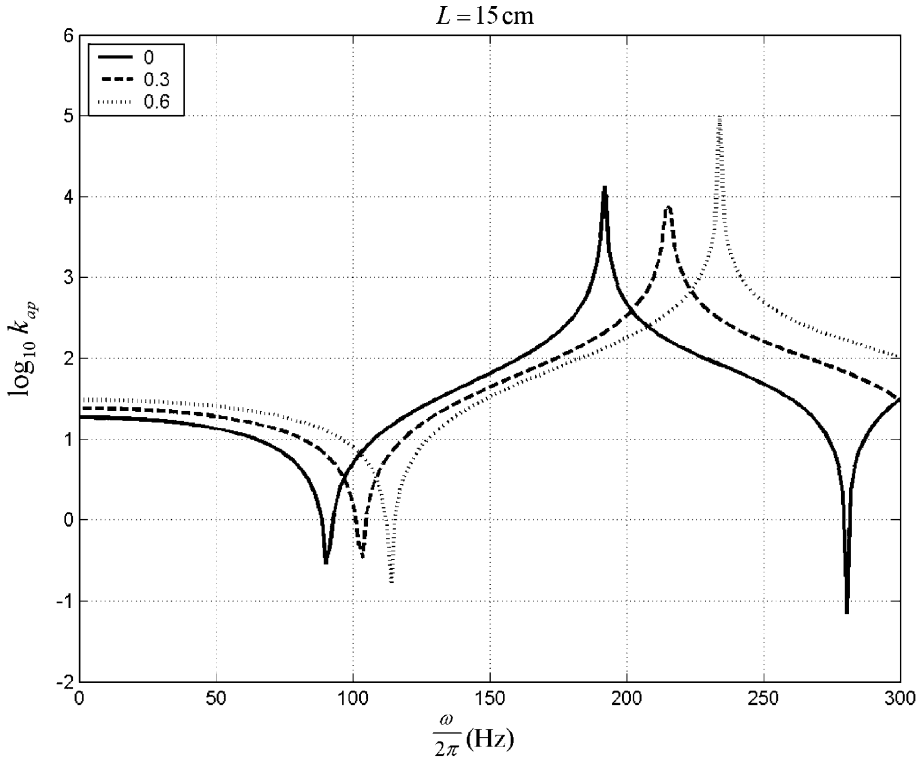

Fig. 3. The apparent stiffness k_{ap} at different shear modulus of MRE for the beam with $L = 15$ cm and $c = 2$ mm.

30%. This characteristic indicates the increase of the applied magnetic field will increase the flexure rigidity of the sandwich beam.

The magnetoelastic loads and the change of the shear modulus of MRE core both affect the dynamic property of the sandwich beam. The following simulation is to reveal the major effect. The size of the sandwich beam is still the same with the above simulation. In Fig. 4, the line marked by pentagon represents the curve of $\log_{10} k_{\mathrm{ap}}$ at $B_0 = 1$ T when the magnetoelastic loads are considered; while the line marked by circle represents the curve of $\log_{10} k_{\mathrm{ap}}$ at $B_0 = 1$ T when the magnetoelastic loads are not considered. From the two curves, it can be seen that the effect of the magnetoelastic loads on the change of the dynamic property of the sandwich beam is very small. Thus, the change of the shear modulus of MRE is the major effect on the increase of the flexure rigidity of the sandwich beam.

Now, the effect of the length of the MRE core on the controllable dynamic property of the sandwich beam will be addressed. The MRE core is centered at the mid-point of the beam because of the symmetry of the configuration. To seek the effect of the length of the MRE core, the flowing index is defined:

$$J\left(\frac{x_r - x_l}{L}, L\right) = \frac{\int_0^{+\infty} \left[k_{\mathrm{ap}}(0.6, \omega) - k_{\mathrm{ap}}(0, \omega)\right]^2 \mathrm{d}\omega}{\int_0^{+\infty} \left[k_{\mathrm{ap}}(0, \omega)\right]^2 \mathrm{d}\omega} \tag{43}$$

J denotes the relative change of the apparent stiffness, k_{ap}, between zero-field shear modulus and maximum field-induced shear modulus of MRE core. This index is a function of the length of the MRE core and the length of the beam and the maximum of this index presents the maximum of the controllability. Thus, this index can be used to reveal the effect of the length of the MRE core on the controllability of the sandwich

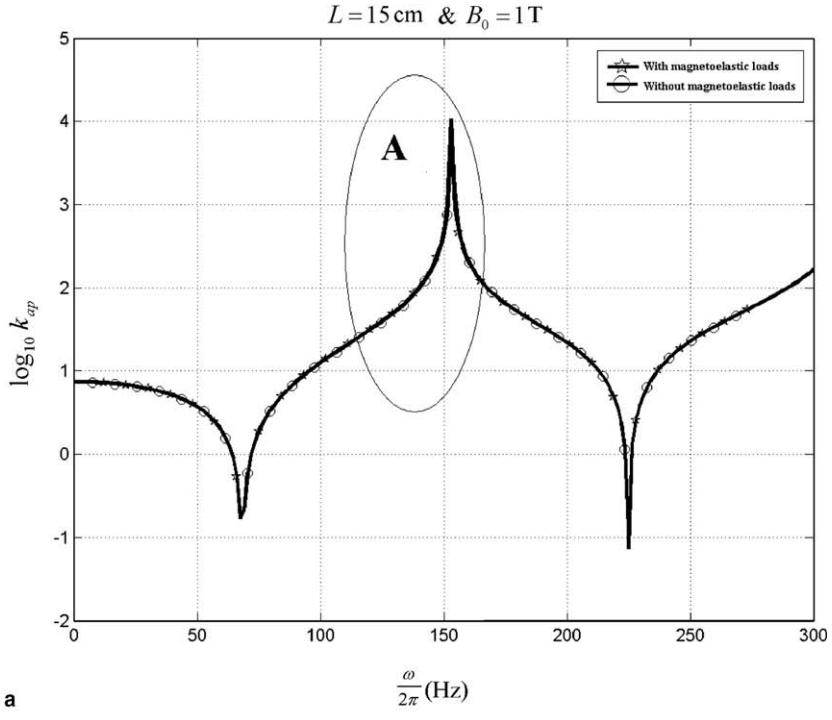

Fig. 4. The effect of the magnetoelastic loads for the proposed sandwich beam with $L = 15\,\text{cm}$ and $c = 2\,\text{mm}$ when $B_0 = 1\,\text{T}$: (a) Panorama; (b) zoom of part A.

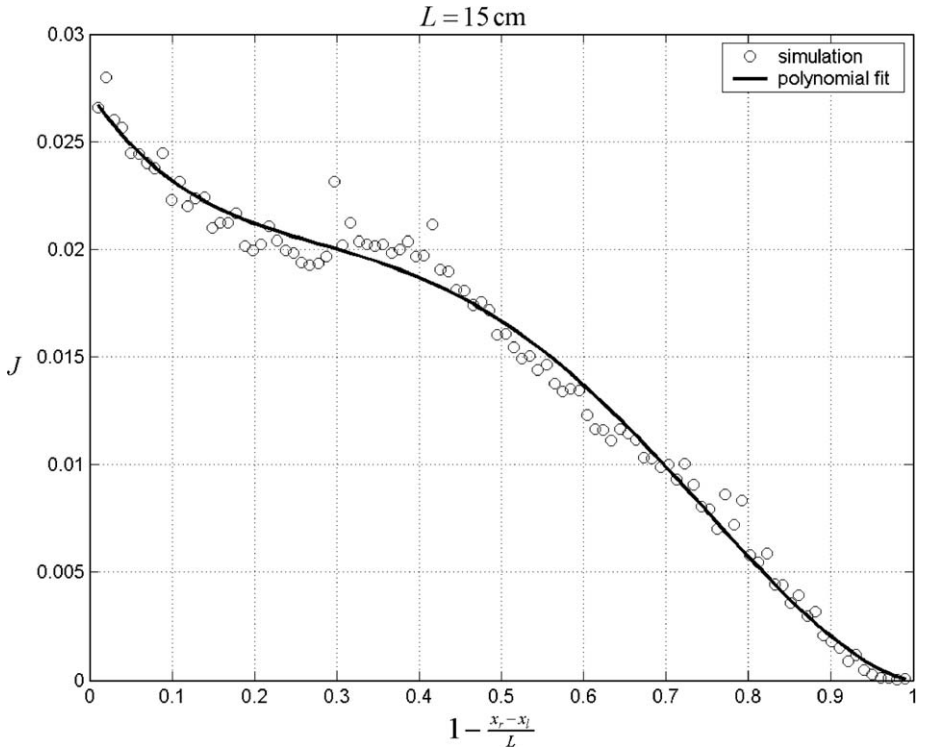

Fig. 5. The MRE-induced relative change of the apparent stiffness curve against the length of the core ($L = 15$ cm and $c = 2$ mm).

beam. In Fig. 5, the curve of J against $L - \frac{x_r - x_l}{L}$ when $L = 15$ cm is given. The fluctuation of the simulation results is caused by only 20 terms in series expression used in Galerkin method. Thus, the simulation results are fitted by a fourth order polynomial. It can be seen J decreases monotonously with $L - \frac{x_r - x_l}{L}$. Thus, the maximum controllability occurs when the MRE core composes the soft core completely. The cases of $L = 10$ cm and $L = 12$ cm are all simulated and the curves of J are all with the above characteristic.

With the above discussion on the effect of the length of MRE core on the controllable property of the proposed sandwich beam, the soft core of the sandwich beam is assumed to be composed of MRE completely in the following simulations. Figs. 6(a) and 7(a) present the distribution of $\log_{10} k_{\mathrm{ap}}$ in the $\gamma_{\mathrm{GMRE}} \sim \frac{\omega}{2\pi}$ domain for the sandwich beam with $L = 10$ cm and $L = 15$ cm respectively. Figs. 6(b) and 7(b) are the corresponding top-views. From the figures, both the anti-resonant frequencies (see the lines marked by the symbol without subscription) and resonant frequencies (see the lines marked by the symbol with the subscription "b") increase with γ_{MRE}. These results reaffirm the increase of the magnetic field will increase the flexure rigidity of the sandwich beam.

4. Conclusions

The dynamic property of a sandwich beam, composed of conductive skins and soft core with both MRE and non-MRE parts, is studied. Due to the controllable shear property of the core and the magnetoelastic loads on the conductive skins, the dynamic performance of the sandwich beam and the stiffness of the beam will be enhanced by the applied magnetic field. According to the analytical solution on magnetoelastic loads

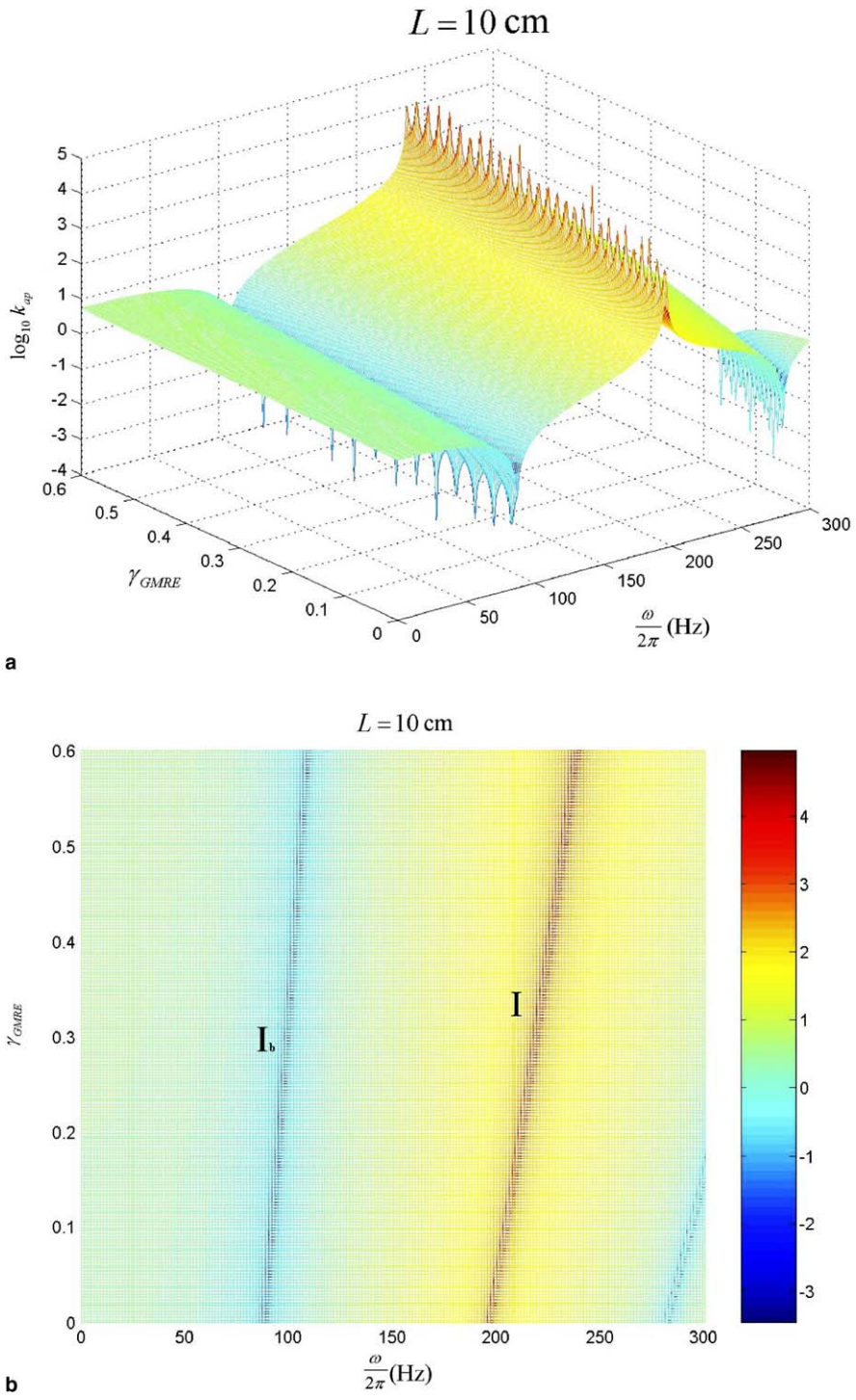

Fig. 6. The distribution of apparent stiffness in the $\gamma_{\mathrm{GMRE}} \sim \frac{\omega}{2\pi}$ domain for the beam with $L = 10$ cm: (a) the 3D distribution; (b) the top-view.

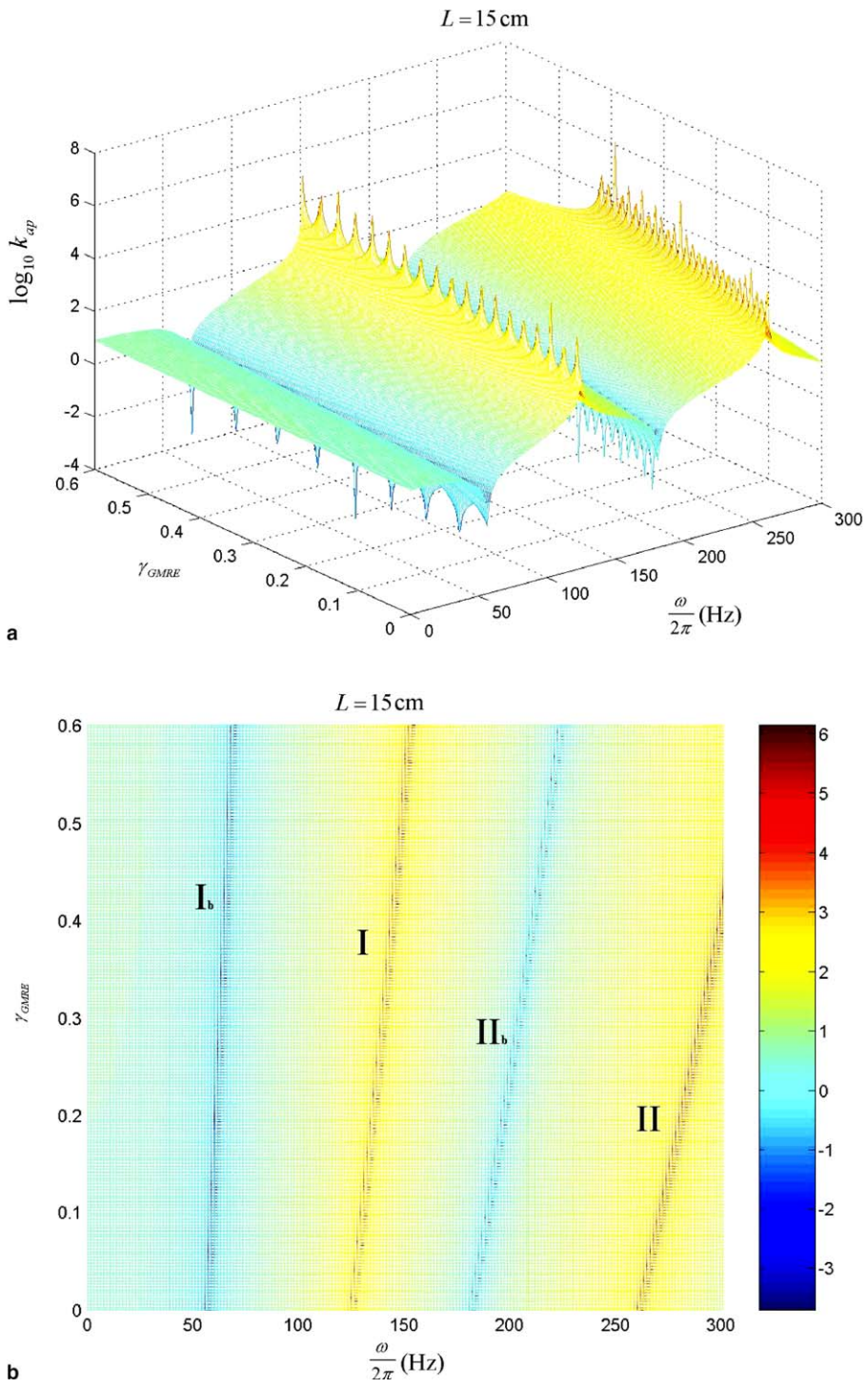

Fig. 7. The distribution of apparent stiffness in the $\gamma_{\mathrm{GMRE}} \sim \frac{\omega}{2\pi}$ domain for the beam with $L = 15$ cm: (a) the 3D distribution; (b) the top-view.

of a thin vibrating beam, the model based on Hamilton principle for the proposed sandwich beam is presented and numerical simulations on a simply supported beam are conducted. In the simulations, the vertical external force on the upper skin distributed in an extremely narrow region around the center of the beam is examined. The apparent stiffness at the center of the beam is utilized to reveal the controllability of the proposed sandwich beam. From simulations, the following conclusions for the beam have been found:

1. For the sandwich beam with high length-thickness ratio, the highest controllability of the sandwich beam occurs when the core is composed of MRE completely.
2. The flexure rigidity of the MRE-based sandwich beam increases with the applied magnetic field.
3. The change of the dynamic property of the sandwich beam is mainly caused by the change of the shear modulus of MRE.
4. The resonant frequencies and anti-resonant frequencies increase with the applied magnetic field up to 30% before magnetic saturation occurs.
5. For the sandwich beam with skins thicker than 0.1 mm, such as the cases in our simulation, the field-induced change of the dynamic property is mainly caused by the field-dependant shear modulus of MRE.

The above conclusions reveal that the proposed sandwich beam exhibits promising controllable property. Since the bulk stiffness of the sandwich can be widely increased by the applied magnetic field, the proposed sandwich beam holds potentials for developing applicable semi-active devices for vibration control.

References

Badolato, A.R., Pawlowski, R.P., 2003. Tunable slip yoke damper assembly. US patent, 6,623,364, September 23.

Bozhevolnaya, E., Frostig, Y., 1997. Nonlinear closed-form high-order analysis of curved sandwich panels. Composite Structures 38 (1–4), 383–394.

Davis, L.C., 1999. Model of magnetorheological elastomers. Journal of Applied Physics 85 (6), 3348–3351.

Demchuk, S.A., Kuzmin, V.A., 2002. Viscoelastic properties of magnetorheological elastomer in the regime of dynamic deformation. Journal of Engineering Physics and Thermophysics 75 (2), 396–400.

Frostig, Y., 1992. Behavior of delaminated sandwich beam with transversely flexible core-high order theory. Composite Structures 20, 1–16.

Frostig, Y., Baruch, M., 1994. Free vibrations of sandwich beams with a transversely flexible core: a high order approach. Journal of Sound and Vibration 176 (2), 195–208.

Ginder, J.M., Nichols, M.E., et al., 1999. Magnetorheological elastomers: properties and applications. In: SPIE Conference on Smart Materials Technologies, vol. 3675, pp. 131–138.

Jolly, M.R., Carlson, J.D., et al., 1996. The magnetoviscoelastic response of elastomer composites consisting of ferrous particles embedded in a polymer matrix. Journal of Intelligent Material Systems and Structures 7, 613–622.

Librescu, L., Hause, T., 2000. Recent developments in the modeling and behavior of advanced sandwich constructions: a survey. Composite Structures 48, 1–17.

Schlotter, W.F. et al., 2002. The dynamics of magnetorheological elastomers studied by synchrotron speckle analysis. International Journal of Modern Physics B 16, 2426–2432.

Shiga, T., Okada, A., et al., 1995. Magnetoviscoelastic behavior of composite gels. Journal of Applied Polymer Science 58 (4), 787–792.

Zhou, G.Y., 2003. Shear property of a magnetorheological elastomer. Smart Materials and Structures 12, 139–146.

Zhou, G.Y., 2004. Complex shear modulus of a magnetorheological elastomer. Smart Materials and Structures 13, 1203–1210.

Zhou, G.Y., Li, J.R., 2003. Behavior of a Magnetorheological Elastomer Under Uniaxial Deformation: I Experiment. Smart Materials and Structures 12, 859–872.

Zhou, G.Y., Jiang, Z.Y., 2004. Deformation in magnetorheological elastomer and elastomer-ferromagnet composite driven by a magnetic field. Smart Materials and Structures 13, 309–316.

Zhou, G.Y., Wang, Q., 2005. Design of smart piezoelectric actuator based on magnetorheological elastomer. Smart Materials and Structures 14, 504–510.

Zhou, G.Y., Wang, Q., in press. Magnetorheological elastomer-based smart sandwich beam with nonconductive skins. Smart Materials and Structures.